ARTICLE   OPEN

Check for updates

Changes in atmospheric oxidants over Arctic Ocean atmosphere: evidence of oxygen isotope anomaly in nitrate aerosols

Yanlin Zhang [1,2 ✉], Zhuyu Zhao [1,2], Fang Cao [1,2], Wenhuai Song[1,2], Yuchi Lin[1,2], Meiyi Fan[1,2], Haoran Yu[1,2], Hanyu Li[1,2], Yihang Hong [2] and Meng Gao [3]

Oxygen isotope anomaly of nitrate aerosol ($\Delta^{17}O\text{-}NO_3^-$) contributes to understanding the atmospheric nitrogen chemistry in the polar oceans. Here, $\Delta^{17}O\text{-}NO_3^-$ of the aerosol samples was analyzed based on a cruise from East Asia to the Arctic Ocean to explore the nitrate formation mechanisms. $\Delta^{17}O\text{-}NO_3^-$ decreased with the increase of latitude, especially when after entering the Arctic Circle. $\Delta^{17}O\text{-}NO_3^-$ (e.g., 11.5‰–21.2‰) was extremely low while crossing the sea ice-covered Arctic Ocean. This is most likely influenced by the combined enhancement of hydroxyl (OH) and peroxy ($HO_2 + RO_2$) radicals derived by sea ice under permanent sunlight period. In addition, the obvious increase in the $\Delta^{17}O\text{-}NO_3^-$ of return trip with shortened daytime indicated the advantage of nocturnal pathways (NO_3 related) with the higher $\Delta^{17}O$ endmembers. The mutation of $\Delta^{17}O\text{-}NO_3^-$ can reflect the change of NO_x conversion pathways to nitrate, and it can be more sensitive to the change of radical chemistry related to atmospheric oxidation.

INTRODUCTION

Atmospheric nitrate aerosols in polar regions can record changes in atmospheric oxidation potential and greatly influence regional atmospheric chemistry[1,2], because the cycle of NO_x and changes in the formation pathway of nitrate aerosols affect the production rate of O_3 and the life of NO_x[3]. Nitrates account for 75–100% of nitrogen emissions deposited from the atmosphere in the Arctic and Antarctic[2]. Numerous studies have well-studied the nitrate formation pathways in terrestrial and coastal areas[4–8]. However, due to observational restrictions and other limitations, the formation mechanism of nitrate in the oceans, especially in the Arctic Circle, is still unclear and needs to be further studied. Nitrate impacts the oxidation capacity of the oceanic atmosphere[9]. In addition, many free radical groups (e.g., HO_2, RO_2, OH, etc.) are involved in the formation process of nitrate[10]. Nitrate is widely recognized as an important factor for understanding the marine geochemical cycle, especially to understand the atmospheric oxidation related to reactive nitrogen[11–13].

During the rapid cycle of NO_x during the day, NO_2 undergoes photolysis and decomposes into NO and atomic oxygen, and then O_3 is generated after the atomic molecular oxygen combines with molecular oxygen[14]. Tropospheric NO is mainly oxidized by O_3 and HO_2/RO_2:

$$NO + O_3 \rightarrow NO_2 + O_2 \tag{1}$$

$$NO + HO_2/RO_2 \rightarrow NO_2 + OH/OR \tag{2}$$
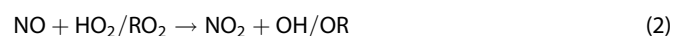
And oxidized halogen XO (X stands for Cl, Br, I) can also be the oxides in certain conditions such as in the air above the open sea:

$$NO + XO \rightarrow NO_2 + X \tag{3}$$

The conversion of NO_x to HNO_3 goes through a series of complex pathways, generally including:

$$NO_2 + OH \rightarrow HNO_3 \tag{4}$$

$$NO_2 + O_3 \rightarrow NO_3 + O_2 \tag{5}$$

$$NO_3 + HC/DMS \rightarrow HNO_3 + \text{other product} \tag{6}$$

$$NO_2 + NO_3 \rightarrow N_2O_5 \tag{7}$$

$$N_2O_5 + H_2O \rightarrow 2HNO_3 \tag{8}$$

Among them, dimethyl sulfide (DMS) are usually produced in the ocean by phytoplankton[15]. Besides, although halogens can be produced by coal combustion on land[16,17], halogen chemistry plays an important role in nitrate formation mainly in the oceans and polar regions[18,19]:

$$NO_2 + XO + M \rightarrow XONO_2 + M \tag{9}$$

$$XONO_2 + H_2O \rightarrow HOX + HNO_3 \tag{10}$$
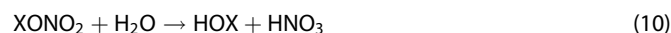
The reaction relating to hydroxyl radical (OH) (Eq. (4)) takes place during the day because the formation of OH requires photolysis. Whereas, due to the photosensitivity of NO_3 radicals, the reaction with NO_3 and N_2O_5 (Eqs. (6) and (8)) proceeds at night. Halogen chemistry may be the main role of tropospheric nitrate formation, especially in the oceanic atmosphere[20].

Oxygen isotope anomaly (expressed as $\Delta^{17}O = \delta^{17}O\text{-}0.52 \times \delta^{18}O$) is a powerful tool to reflect the mechanism involved in the formation of nitrate, which contributes to a better understanding of the atmospheric nitrogen cycle[6,9,18,21,22]. Different oxidants (O_3, OH,

[1]School of Applied Meteorology, Nanjing University of Information Science and Technology, Nanjing 210044, China. [2]Atmospheric Environment Center, Joint Laboratory for International Cooperation On Climate and Environmental Change, Ministry of Education, Nanjing University of Information Science and Technology, Nanjing 210044, China. [3]Department of Geography, State Key Laboratory of Environmental and Biological Analysis, Hong Kong Baptist University, Hong Kong SAR, China. ✉email: zhangyanlin@nuist.edu.cn

HO$_2$/RO$_2$, XO) containing different Δ^{17}O are involved in the different reaction pathways, leading to different Δ^{17}O of HNO$_3$[23] (Supplementary Note 1). O$_3$ and XO (ozone oxidation product) have high Δ^{17}O values, while the Δ^{17}O of other oxidants (HO$_2$/RO$_2$ and OH) are low and can basically be ignored[24]. This means that nitrate produced through NO$_3$ + HC (Eq. (6)) and XONO$_2$ hydrolysis (Eq. (10)) pathways has the highest Δ^{17}O, followed by N$_2$O$_5$ hydrolysis (Eq. (8)), and nitrate produced through NO$_2$ + OH (Eq. (4)) pathway has the lowest Δ^{17}O value (quantification are shown in Methods). Because Δ^{17}O is mass-independent, it doesn't undergo isotopic fractionation during the conversion, therefore Δ^{17}O can identify the conversion pathway of NO$_x$ from different pathways to nitrate more accurately.

Li et al.[25] recently reported the changes in the source and formation mechanism of atmospheric nitrate based on isotopes during the two cruises from Shanghai, China to the Arctic Ocean in 2017 and 2018. This provides strong support for enhancing our understanding of the N cycle of the oceanic atmospheric boundary in the Arctic region. Before their study, almost all the reported Δ^{17}O-NO$_3^-$ was above 20‰ in atmospheric particulate matter in the oceans and polar regions (Supplementary Table 1). In these two cruises, Δ^{17}O of atmospheric nitrate was significantly lower in the high-latitude ocean (70 ~ 85°N, average Δ^{17}O-NO$_3^-$ = 20.3‰, with a minimum value of 14.8‰) than in other lower oceans (30 ~ 50°N: average 27.7‰, 50 ~ 70°N: average 30.5‰). Such a low Δ^{17}O-NO$_3^-$ (mean: 20.3‰) in the high-latitude ocean was attributed to the high contribution of the NO$_2$ + OH (P1) pathway. However, some extremely low values (e.g., 14.8‰) remained unexplored as these values have been already below the lowest limit of the Δ^{17}O-NO$_3^-$ produced by the NO$_2$ + OH pathway (19.8‰) in the study of Li et al.,[25] which requires further investigation. Such anomalous Δ^{17}O-NO$_3^-$ of atmospheric particulate matter has been observed in an altitude station over Taiwan, China (2.7–31.4‰)[26], which is due to that peroxy radical dominated the NO oxidation reaction to NO$_2$. Low Δ^{17}O-NO$_3^-$ values were also observed in precipitation samples over the Tibetan Plateau (6.6–24.1‰)[27], which may be due to the low end member of Δ^{17}O-O$_3$, the decrease of O$_3$ concentration and the increase of hydroxyl and peroxy radicals. In addition, Alexander et al.[28] used the GEOS-Chem model to simulate a global surface Δ^{17}O-NO$_3^-$ range of 4‰ to 33‰, with the lowest values in Amazon areas, which may be caused by the hydrolysis of alkyl nitrate. However, the cause of those low values (< 20‰) for the high Arctic regions remains a puzzle.

We also found a lot of low values in the Arctic Ocean at high latitudes during the expedition of the Chinese R/V Xuelong from East Asia to the Arctic Ocean in 2017. It shows that the lower Δ^{17}O-NO$_3^-$ is not a random event, then it suggests that there are special mechanisms affecting nitrate formation in the high Arctic Ocean and those areas mentioned above. Therefore, in this study, we tried to solve the unexplored mechanism for the lower Δ^{17}O-NO$_3^-$ in the high-latitude Arctic Ocean, using the cruise data with higher temporal and spatial resolution. TSP samples with a resolution of 48 h were collected during the expedition of the Chinese R/V Xuelong from East Asia to the Arctic.

RESULTS AND DISCUSSION
Spatial variation of atmospheric NO$_3^-$ and Δ^{17}O-NO$_3^-$
During the entire R/V Xuelong cruise, the concentration of atmospheric nitrate ranged from 0.03 μg m^{-3} to 1.07 μg m^{-3} (Fig. 1), with apparent spatial characteristics. The NO$_3^-$ concentration decreased with increasing latitude, with the highest level in eastern Asia and the lowest level in the open ocean of the Arctic Ocean (Fig. 2), which is consistent with the results of other Chinese Arctic expeditions[29]. This may show the effect of atmospheric nitrogen input over East Asia on

marine nitrate aerosols. A much higher concentration of NO$_3^-$ was found near the continent (Fig. 2), just like the observations from East Asia to the Antarctic[22]. The concentration of atmospheric NO$_3^-$ inside the Arctic Circle (0.08 ± 0.05 μg m^{-3}) was significantly lower than that outside the Arctic Circle (0.45 ± 0.37 μg m^{-3}). The NO$_3^-$ concentration inside the Arctic Circle is in line with the NO$_3^-$ concentration (0.04 ± 0.02 μg m^{-3}) reported by Morin et al.[30] at the Arctic from June to October and such concentration is thought to indicate less exposure to anthropogenic NO$_x$[31]. Vicars et al.[32] reported the average NO$_3^-$ concentration in the atmosphere (0.52 ± 0.32 μg m^{-3}) on the central coast of the Pacific, and this concentration is regarded as the critical value of the ocean boundary layer in the coastal area of the Pacific free from being subjected to anthropogenic emissions. During the whole cruise, the concentrations of atmospheric NO$_3^-$ of all seas, except for those near East Asia, were consistently below the specified range, while the air mass back trajectories (Supplementary Fig. 1) for the sea areas near East Asia passed over the eastern Asian continent. This suggests the coastal seas of the East Asian continent are more vulnerable to anthropogenic emissions whereas the remote open ocean is less polluted far out than near continental sea. The distribution of other components of the WSI components (Supplementary Fig. 2 and Supplementary Table 2) of TSP had similar spatial distribution characteristics with nitrate, showing higher concentrations outside the Arctic Circle than that inside the Arctic Circle. The composition of WSI in the Arctic Ocean was significantly different
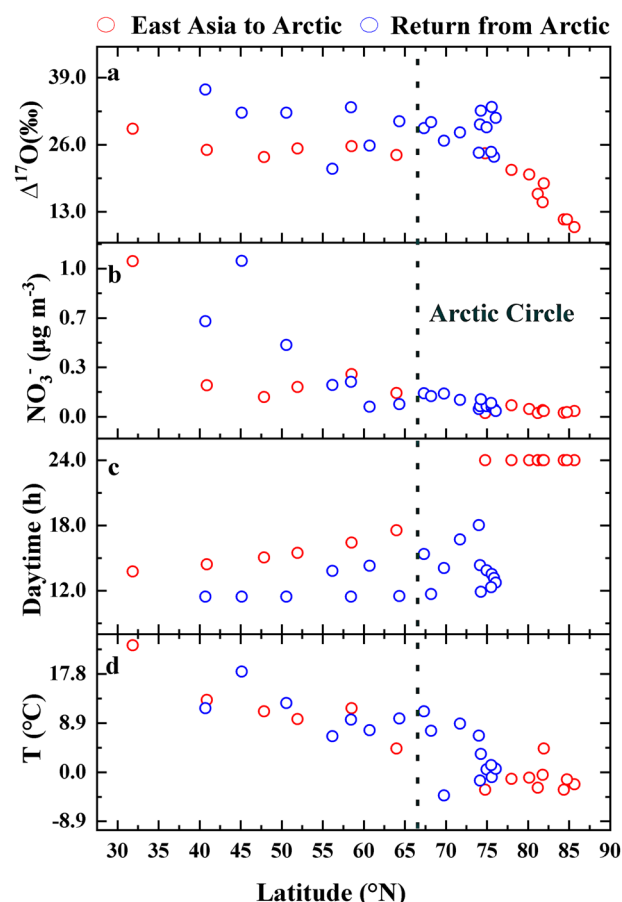

Fig. 1 The evolution of nitrate and its oxygen isotope anomaly over latitudes. The variation series of (**a**) oxygen isotope anomaly of nitrate (Δ^{17}O-NO$_3^-$), (**b**) mass concentrations of nitrate (NO$_3^-$), (**c**) daytime length, and (**d**) temperature with latitude during the R/V Xuelong cruise from East Asia to the Arctic Ocean. The dotted line represents the location of the Arctic Circle. The red dots indicate the outward voyage to the Arctic, and blue dots indicate the return leg.
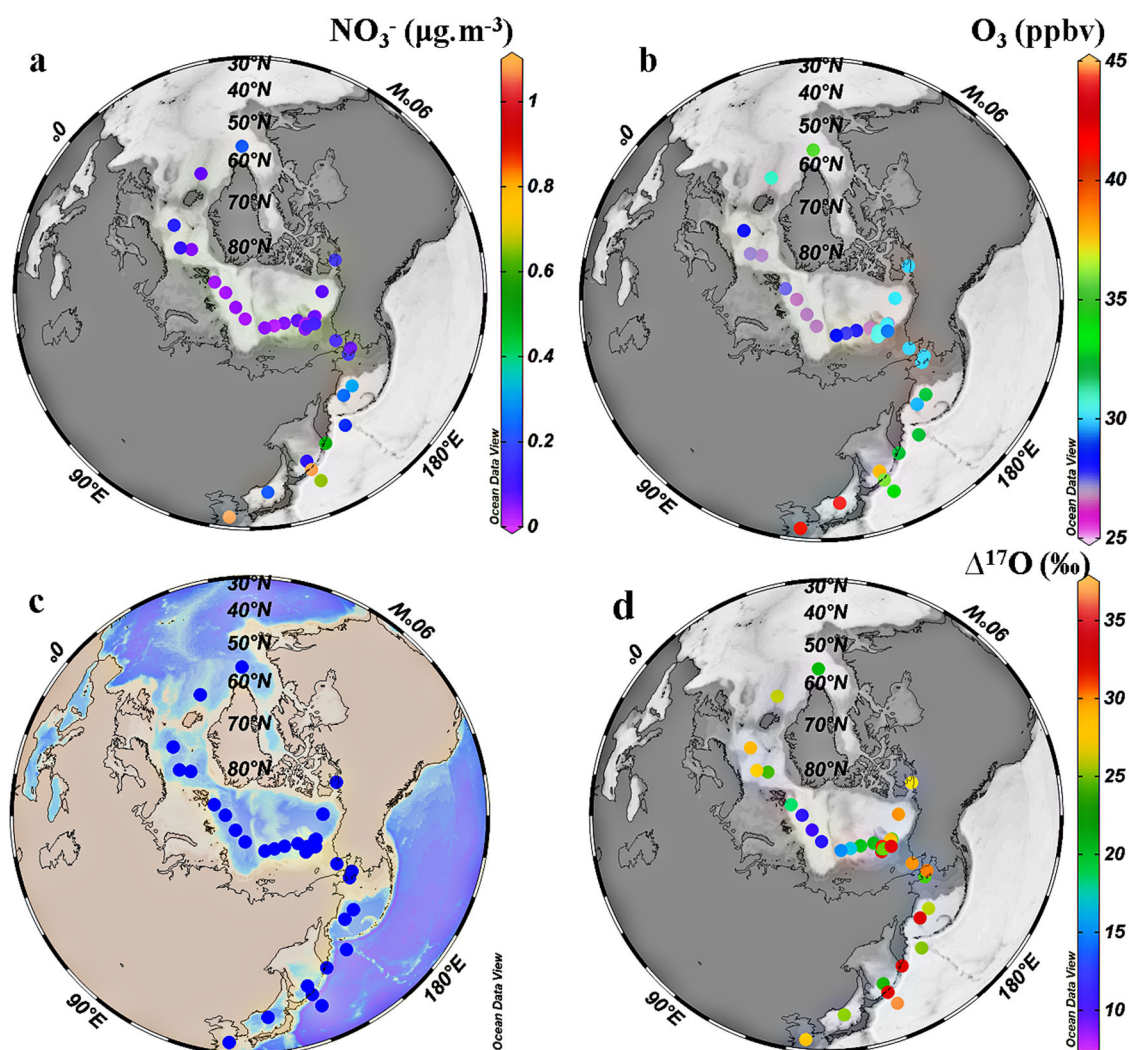
Fig. 2 The distribution of nitrate and its oxygen isotope anomaly. The spatial distribution of (**a**) mass concentrations of nitrate (NO_3^-), (**b**) volume concentrations of ozone (O_3), (**c**) sampling points, (**d**) oxygen isotope anomaly of nitrate ($\Delta^{17}O$-NO_3^-) during the R/V Xuelong cruise from East Asia to the Arctic Ocean.

from that of the coastal oceans of East Asia. Cl^- and Na^+ were the dominant component of WSI in the Arctic Ocean, which also was shown in the Arctic Ocean aerosol WSI of Yu et al.[29]. The results indicate that the contribution of sea salt aerosol to the aerosol composition in the Arctic Ocean is higher than that in the lower latitudes. However, the WSI of aerosol dominated by SO_4^{2-} in the East Asian ocean may show the influence of anthropogenic emissions. The concentration of non-sea-salt sulfate (nss-SO_4^{2-}), mainly from the oxidation of dimethyl sulfide (DMS)[33] emitted by ocean phytoplankton and the discharge of anthropogenic sources especially fossil fuel combustion[34] in the northern hemisphere, was calculated (Supplementary Note 2). The concentrations of nss-SO_4^{2-} (Supplementary Table 2) in the Arctic Circle (0.12 ± 0.11 µg m^{-3}) was significantly lower than out the Arctic Circle (1.86 ± 3.27 µg m^{-3}). Methane sulfonic acid (MSA, mainly comes from oxidation products of DMS in summer[35]) can help to separate the nss-SO_4^{2-} from other sources. The ratio of MSA to nss-SO_4^{2-} was higher inside the Arctic Circle (0.23 ± 0.66) than outside the Arctic Circle (0.06 ± 0.09), indicating that the nss-SO_4^{2-} from the contribution of anthropogenic source was obviously higher than that of low latitude area[36].

During the cruise period, $\Delta^{17}O$-NO_3^- ranged from 11.5‰ to 36.7‰ (Fig. 1). The $\Delta^{17}O$-NO_3^- values were relatively higher when the cruise approached the continent and were lower when approaching open sea (Fig. 2). This suggests that nitrate formation

mechanisms vary with the changing of the land-based emissions, which is consistent with the research in the tropical Pacific Ocean by Carter et al.[11]. They also found high $\Delta^{17}O$-NO_3^- values near continents, and they expected that $\Delta^{17}O$ was much lower for NO_3^- from marine sources compared to the continent. The change of O_3 concentration also followed this spatial distribution characteristics, with higher concentrations near the continent and lower concentrations in the open ocean of the Arctic Ocean (Fig. 2). The difference of atmospheric nitrate $\Delta^{17}O$-NO_3^- in different sea areas may be caused by the different dominant species of main oxidant in the atmosphere, and O_3 dominant area will lead to the formation of nitrate with high $\Delta^{17}O$-NO_3^-. Besides, compared to the open ocean, the concentration of volatile organic compounds (VOCs) including HC in the polluted continents may be higher, due to the presence of more land plants and human-caused emission sources. This will cause high $\Delta^{17}O$ ($NO_3 + HC$/DMS, Supplementary Table 3) in the near-continental oceans.

The $\Delta^{17}O$-NO_3^- is significantly correlated with latitude ($r = -0.54$, $p < 0.01$) during the entire cruise. Besides, the $\Delta^{17}O$ of return stages from the Arctic Ocean (29.3 ± 4.0‰) was significantly higher than the $\Delta^{17}O$ from the Western Pacific to the Arctic Ocean (20.2 ± 5.8‰) ($p < 0.01$). Further, the whole cruise is divided into several stages, and the relationship of $\Delta^{17}O$-NO_3^- with latitude is shown in Fig. 3. Stages I and II represent the cruise
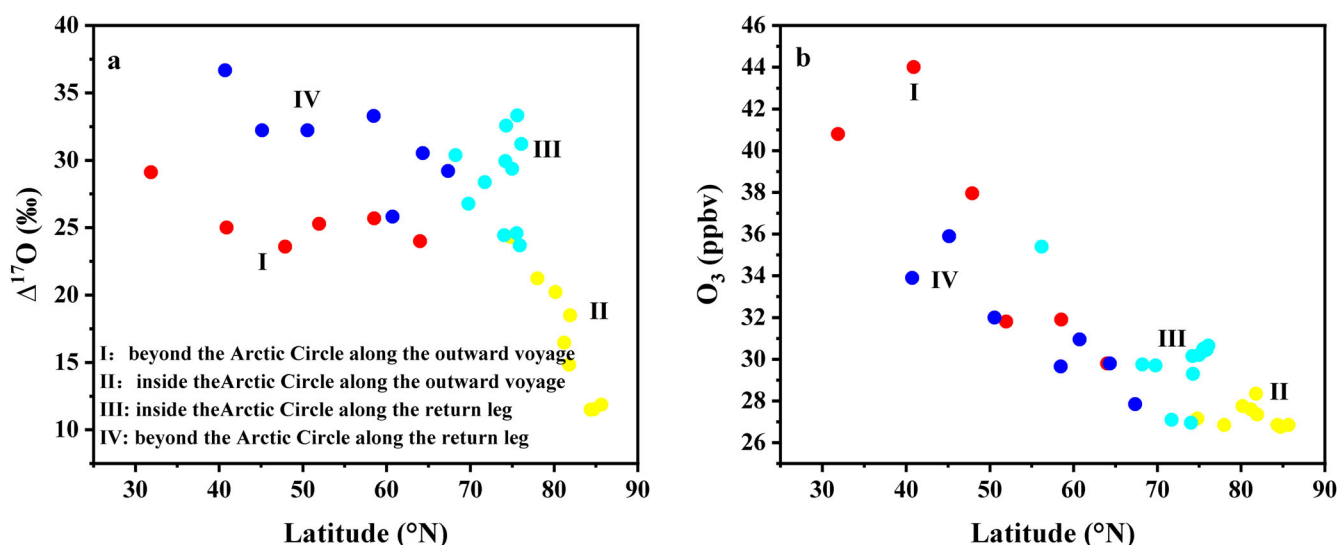
Fig. 3 The variation of oxygen isotope anomaly of nitrate and ozone at different stages. Series of (**a**) oxygen isotope anomaly of nitrate (Δ^{17}O-NO$_3^-$) and (**b**) volume concentrations of ozone (O$_3$) at different stages including stage I (beyond the Arctic Circle along the outward voyage, red dots), II (inside the Arctic Circle along the outward voyage, yellow), III (inside the Arctic Circle along the return leg, green), and IV (beyond the Arctic Circle along the return leg, blue) varying with latitude, respectively.

from East Asia to the Arctic Circle in July-August, and III and IV represent the return cruise in September. Overall, the Δ^{17}O of return stages III and IV were significantly higher than stages I and II (Fig. 3a). However, no significant increase in O$_3$ concentration during the return trip indicates that the changing Δ^{17}O may be not caused by O$_3$ related processes alone (Fig. 3b). This suggests that factors other than dominant oxidants and continental emissions may play a role in the formation of oceanic atmospheric nitrates.

Surprisingly, during the high-latitude ocean while crossing the Arctic Ocean, Δ^{17}O decreased sharply with increasing latitude (Fig. 3, stage II). Possibly due to the high temporal resolution of the observations in this study, more abnormally low Δ^{17}O-NO$_3^-$ values were observed in this study than in the report by Li et al.[25] at high-latitude Arctic Ocean. In the ocean at 80°N to the north, the average value of Δ^{17}O was 14.8 ± 4.1‰, with a minimum of 11.5‰. This further indicates that the appearance of low Δ^{17}O-NO$_3^-$ in the high-latitude Arctic Ocean is not accidental. These low Δ^{17}O-NO$_3^-$ values in stage II corresponded to permanent sunlight period (Supplementary Fig. 3), which suggests that there must be an unknown mechanism of nitrate formation at this stage.

NO$_3^-$ formation mechanisms during the permanent sunlight
As mentioned above, phase II (Fig. 3) in the Arctic Circle corresponded to the Arctic permanent sunlight period, and it had the lowest Δ^{17}O-NO$_3^-$ values (11.5‰–24.3‰, with an average of 16.7 ± 4.7‰) currently observed in the ocean. This was unexpected because previous studies on nitrate formation of the Arctic have mentioned the role of halogens, which would result in high Δ^{17}O-NO$_3^-$ values. Morin et al.[19,37] reported for the first time the Δ^{17}O-NO$_3^-$ in the Arctic, including the permanent sunlight period in the Arctic, and found that the range of Δ^{17}O in spring was 29–35‰. This high Δ^{17}O-NO$_3^-$ value is due to ozone depletion events (ODEs) caused by oxidizing halogens. ODEs are frequently observed in the Arctic spring[38], and are associated with the release of large amounts of bromine radicals[39]. In addition, Morin et al.[30] also monitored the Δ^{17}O-NO$_3^-$ of the Arctic for the whole year, which is probably between 25‰ and 32‰. Even though it is in summer permanent sunlight time, the Δ^{17}O-NO$_3^-$ value is also beyond 25‰, which cannot explain the lowest value (10–20‰) of the Arctic in this study. Firstly, as conventionally thought, the low Δ^{17}O-NO$_3^-$ value at stage

II is due to the dominance of the NO$_2$ + OH (P1) pathway, after all, there should be no nocturnal pathway (NO$_3$–related pathway) in the daytime with permanent sunlight exposure. Moreover, Δ^{17}O-NO$_3^-$ with lower values is often associated with the NO$_2$ + OH pathway. During permanent sunlight with strong UVB exposure, polar OH can come from the photolysis of O$_3$, CH$_2$O, HONO, and H$_2$O generated by the photolysis of ice and snow. But the increase in OH alone is not sufficient to explain the lowest Δ^{17}O in this study. After calculating according to the end members of Δ^{17}O-NO$_3^-$ produced by each pathway in this study (Methods, Supplementary Table 3 and Supplementary Note 1), the Δ^{17}O-NO$_3^-$ of NO$_2$ + OH (P1), NO$_3$ + HC/XONO$_2$ hydrolysis (P2) and N$_2$O$_5$ heterogeneous (P3) was 19.3‰–21.6‰, 31.8‰–34.1‰, and 25.5‰–27.8‰, respectively. According to the end members of Δ^{17}O-NO$_3^-$ produced by NO$_2$ + OH (P1) (19.3‰–21.6‰), even though we hypothesized that the NO$_2$ + OH pathway dominated the formation of nitrate in the permanent sunlight period, however, the observed Δ^{17}O-NO$_3^-$ value of 16.7 ± 4.7‰ was lower than the lowest limit Δ^{17}O-NO$_3^-$ of the NO$_2$ + OH pathway. Therefore, it is speculated that exists a special process that makes our conventional calculation of the Δ^{17}O value of the nitrate formation mechanism higher than the actual situation. And this particular process should have a clear variation with latitude, which caused the sharp decrease of Δ^{17}O-NO$_3^-$ with increasing latitude in phase II. Interestingly, we found that phase II fit perfectly with passing through the sea ice cover area. As shown by the sea ice concentration modeled by Nimbus-7 SMMR and DMSP SSM/I-SSMIS Passive Microwave Data V002 (https://search.earthdata.nasa.gov/) in Fig. 4, the permanent sunlight period of phase II corresponded to passing through the sea ice, which is consistent with the sea ice prediction results of Mu et al.[40] for the same batch of R/V Xuelong cruise. Moreover, the sea ice concentration has the characteristics of being higher near the pole. Therefore, the lowest Δ^{17}O-NO$_3^-$ during phase II and the sharp decline with increasing latitude (Fig. 3) may be attributed to the sea ice derived changing of atmospheric oxidation.

Sea ice may affect the formation mechanisms of atmospheric nitrate in two ways. One of them is that the NO$_x$ produced by the photolysis of nitrate in ice and snow re-participates in the formation of atmospheric nitrate, and the other is that atmospheric chemical processes derived from sea ice may release free radicals associated with nitrate formation processes, altering local atmospheric oxidation. Nitrate is known to be one of the most
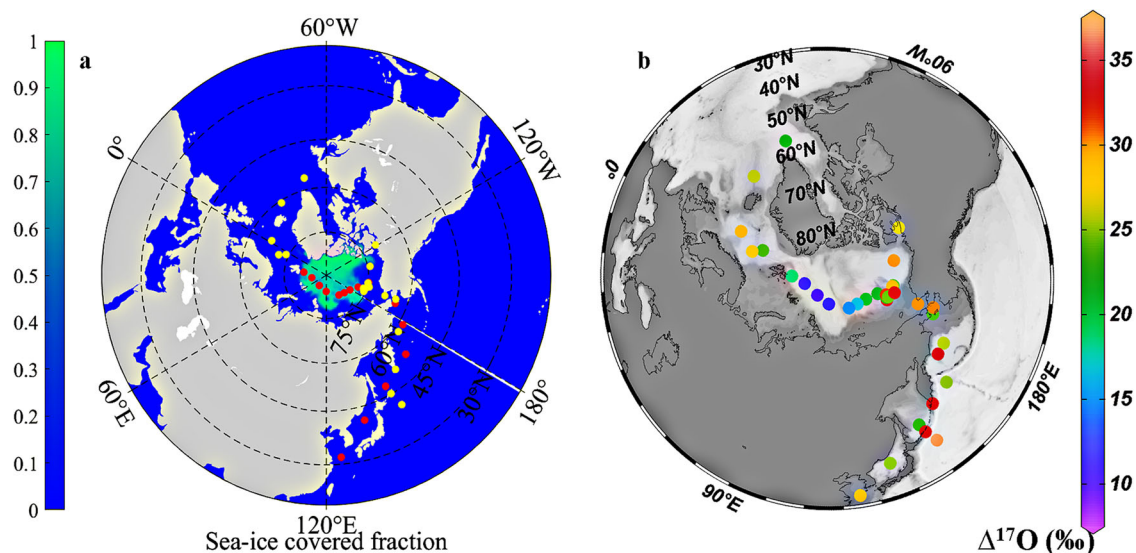
Fig. 4 Distribution of Arctic sea ice. The spatial distribution of (**a**) sea ice covered fraction and (**b**) oxygen isotope anomaly of nitrate ($\Delta^{17}O\text{-}NO_3^-$) during the R/V Xuelong cruise. The red and yellow dots on **a** indicate sampling sites over the outward voyage to the Arctic, and the return leg, respectively.

important ions in polar ice and snow[41]. The photolysis of nitrate has to be considered when it comes to ice and snow. Contaminant/nutrient sources from mid-to-high latitudes can be deposited on sea ice as wet or dry deposition and incorporated into the ice matrix. Therefore, the release of reactive nitrogen from melting snow and ice may be important during the melt season. Aerosol $\Delta^{17}O\text{-}NO_3^-$ may be reduced if affected by the photolysis of nitrates in ice and snow[42]. It is assumed that the $\Delta^{17}O$ value of NO_x produced by photolysis of ice and snow will be low, and NO_2 is the main product of nitrate photolysis[43], so NO_2 with low $\Delta^{17}O$ generates nitrate through various pathways, which may lead to lower $\Delta^{17}O\text{-}NO_3^-$. Morin et al.[30] reported one-year $\delta^{15}N\text{-}NO_3^-$ observed at the Arctic Alert site (82.5°N), and summer $\delta^{15}N\text{-}NO_3^-$ was highest ($-1\permil$ on average) due to the least effect of nitrate emissions from snow, while $\delta^{15}N\text{-}NO_3^-$ in spring had very low values matching the Antarctic summers, which has been attributed to snow photolysis. Berhanu et al.[41,44] estimated that $\delta^{15}N$ isotope fractionation associated with snow NO_3^- photolysis in Antarctica ranged from $-47.9\permil$ to $-55.8\permil$. This isotope fractionation will result in very low $\delta^{15}N$ of NO_x from photolysis, which in turn results in very low $\delta^{15}N$ of aerosol NO_3^-. However, in this study, the $\delta^{15}N$ value corresponding to the permanent sunlight period was $-3.4 \pm 1.6\permil$, which is much higher than the value caused by snow photolysis. Furthermore, Clark et al.[45] reported that $\delta^{15}N\text{-}NO_3^-$ did not show very lower values in the Arctic open ocean from previous Antarctic ice and snow sources in the summer study, and surface snow samples did not behave any significant direct evidence of NO_3^- photolytic loss. This indicates that the recovered snow-derived NO_x is not a significant source of atmospheric nitrate in the summer Arctic ocean. So the lowest $\Delta^{17}O\text{-}NO_3^-$ while crossing sea ice-covered sea during the permanent sunlight phase could not be explained by the effect of NO_3^- photolysis in snow and ice.

Burger et al.[31] observed very low $\delta^{18}O\text{-}NO_3^-$ ($\delta^{18}O\text{-}NO_3^-$ of half sample is less than 31‰) in the Weddle Sea in the Southern Hemisphere, and this is due to the effect of sea ice emissions, which can enhance the production of RO_2. Brough et al.[46] observed an increase in $HO_2 + RO_2$ concentration when air masses arrived from sea ice cover in the Antarctic coastal region in spring because sea ice provides a source of halogen radicals such as Cl and Br. Cl can generate R through the reaction of $RH + Cl \rightarrow R + HCl$, and then $R + O_2 \rightarrow RO_2$. This reaction is important in the Arctic[47].

Besides, the presence of Br can increase the concentration of OH and RO_2[48] through the reaction with O_3 to form BrO, then BrO reacts with H_2O_2 to generate HOBr, which in turn can be photolysis to generate OH. Brough et al.[46] showed that air masses passing through sea ice regions had higher OH concentrations in the study on the Antarctic coast and that the co-existence of sea ice and sunlight may lead to increased OH concentrations. The increase in OH concentration during the permanent sunlight period can also enhance the generation of peroxy radicals ($CO + OH \rightarrow CO_2 + HO_2$, $RH + OH \rightarrow H_2O + RO_2$)[49]. Therefore, the low $\Delta^{17}O\text{-}NO_3^-$ value during permanent daylight can be attributed to the combined contribution of the HO_2/RO_2 and OH radicals. Among them, HO_2/RO_2 is the most important, because that Geng et al.[42] also suggested that $\Delta^{17}O\text{-}NO_3^-$ value is mainly sensitive to the relative abundance of O_3 and $HO_2 + RO_2$, while only changing the $OH + NO_2$ pathway has relatively little effect on $\Delta^{17}O\text{-}NO_3^-$. The increase of HO_2/RO_2 may result in a very large proportion of NO_2 generated by HO_2/RO_2 oxidation relative to O_3, which also implies an overestimation of the value of estimated A (Supplementary Note 1). This would then result in an over-estimation of the end members of $\Delta^{17}O\text{-}NO_3^-$ for each pathway. Our estimated $HO_2 + RO_2$ in the permanent sunlight period was around 10pptv, which is similar to the results previously observed in Greenland (8.4pptv) in the Arctic[50]. Although Morin et al.[51] think that the value of A depends on the mixing ratio of O_3, if sea ice causes a large increase in $HO_2 + RO_2$ in the permanent sunlight period, the value of A is likely to decrease greatly. The value of A in stage II was estimated to be 0.78 ± 0.01 (Supplementary Fig. 4), and the lowest value of the $NO_2 + OH$ (P1) pathway was calculated to be 19.3‰. Similarly, Li et al.[25] attributed the observed low $\Delta^{17}O\text{-}NO_3^-$ values in the high latitude Arctic ocean to the $NO_2 + OH$ pathway, but based on their calculation of the A value (0.76) and their assumption for $O_3^*(26 \times 1.5)$, the lower limit of $\Delta^{17}O\text{-}NO_3^-$ (19.8‰) for the $NO_2 + OH$ pathway is also much higher than the observed lowest value of 14.8‰. Therefore, to match these low $\Delta^{17}O\text{-}NO_3^-$ values, the A value of phase II must be higher than currently estimated. When the concentration of HO_2 and RO_2 is doubled (20pptv), the A value can be reduced by about 0.2, which would be similar to the simulation of the A value (around 0.5) in glacial-interglacial period by Geng et al.[42]. Then, the theoretical end members of $\Delta^{17}O\text{-}NO_3^-$ value of the P1 pathway at stage II will change from 19.3‰ to 12.5‰. When the A

value decreased by 0.2 and 0.4, the mean value of the P1 pathway decreased by 25.7% and 51.3%, respectively. If A = 0.5 was used in stage II, the SIAR quantitative analysis of nitrate formation pathways showed that $88.8 \pm 9.4\%$ nitrate was produced by $NO_2 + OH$ (P1) and $11.2 \pm 9.4\%$ by $BrONO_2$ hydrolysis of P2 (Supplementary Figure 5b). Therefore, a complex reaction of peroxy radical generation is possible for this period of permanent sunlight and in the sea ice-covered sea, but it is not possible to discuss it in depth in this study due to the lack of measurement of peroxy radical concentration. Evidence for an increase in peroxy radicals in the atmosphere covered by Arctic sea ice remains limited and further research is needed.

Different nitrate formation mechanisms in the return cruise

The increasing trend of $\Delta^{17}O$ on the return journey is in line with the shortening of the length of the daytime. There is a very significant negative correlation ($r = -0.85$, $p < 0.01$) relationship between daytime length and $\Delta^{17}O$ values (Supplementary Fig. 6). The cruise was mostly carried out in July to September, corresponding to the Northern hemisphere summer, therefore, the higher the latitude, the longer the daytime. The day length of stages I, II, III and IV was 15.4 ± 1.4 h, 24 h, 14.0 ± 1.9 h and 11.5 ± 1.3 h, respectively. The increased nighttime on the return trip (III and IV) may make pathways for high $\Delta^{17}O\text{-}NO_3^-$ values associated with NO_3 and N_2O_5 ($NO_3 + HC/DMS$ of P2 and P3) more important. When longer daytimes occurred in stages I and II, the decrease in $\Delta^{17}O$ (Fig. 3a) also indicated an increase in the proportion of diurnal pathways $NO_2 + OH$ (P1). For stages I and IV in the ocean with almost the same latitude outside the Arctic Circle, the mean $\Delta^{17}O$ was 25.7‰ and 32.5‰, respectively. Combined with the SIAR results of quantitative estimates of nitrate pathways (Supplementary Fig. 5a, d), nitrate in stages I and IV should be mainly generated by $NO_2 + OH$ pathway ($38.9 \pm 11.8\%$) (P1) and $NO_3 + HC/DMS$ or $XONO_2$ hydrolysis ($47.4 \pm 17.0\%$) (P2), respectively. In other words, the increase of $\Delta^{17}O\text{-}NO_3^-$ in return stage IV is mainly caused by the increase of P2 pathway and the decrease of P1 pathway. The nitrate formation mechanism in the non-permanent sunlight period (stage III) inside the sea area of the Arctic Circle during the return journey (Supplementary Fig. 5c) also changed significantly compared with the permanent sunlight period (stage II) during the journey from Asia to the Arctic (Supplementary Fig. 5b). That is, the length of daytime significantly affects the mechanism of nitrate formation in oceanic atmosphere. Surprisingly, N_2O_5 heterogeneous pathway (P3) did not change significantly in stage I and stage IV (Supplementary Fig. 5a, d), indicating that the $NO_3 + HC/DMS$ pathway may be more important than the N_2O_5 heterogeneous hydrolysis pathway in the marine atmosphere. Study has shown that the NO_x sink of N_2O_5 in a relatively clean environment is significantly reduced[3], which may be due to insufficient NO_x reacting with NO_3 to form N_2O_5, and the concentration of aerosols may be lower than in polluted areas, so there would be not enough surface for heterogeneous reactions with N_2O_5. Although the $NO_3 + HC$ and $BrONO_2$ hydrolysis pathways of P2 could not be distinguished, we attribute the high contribution of P2 in return stage to the $NO_3 + HC/DMS$ pathway, as the nitrate production via nocturnal NO_3–related pathways may increase as nights get longer. This does not mean the unimportant of halogen $BrONO_2$ hydrolysis pathway, but there is no evidence that this pathway has a good trend with latitude or day length. The previous studies in the Arctic reported a very high contribution of the $BrONO_2$ hydrolysis pathway to nitrate formation in the context of ozone depletion events (ODEs)[19,30]. Brominated compounds, mainly from sea salt, catalyzed the destruction of boundary layer ozone. In our study, there was no sudden decrease in O_3 concentration (Figs. 2, 3b) in Arctic sea areas, which could be because O_3 depletion events mostly occurred in the arctic spring[52]. Savarino et al.[3] showed that

the $NO_3 + DMS$ and $BrONO_2$ hydrolysis pathways (P2) in the tropical ocean boundary layer can account for about 40% and 20%, respectively. Shi et al.[22] showed that the contribution of the $BrONO_2$ hydrolysis pathway in the ocean increases toward the Antarctic in the cruise from East Asia to Zhongshan Station in Antarctica. $BrONO_2$ hydrolysis pathway has been shown to contribute significantly to the formation of nitrate in the Pacific and Atlantic oceanic boundary layers[18]. It can be seen that the role of halogens can not be ignored in the study of the formation mechanism of marine atmospheric nitrate, but considering the contribution of the halogen nitrate hydrolysis pathway during the permanent sunlight day (~10 %), the contribution of this pathway to marine atmospheric nitrate in this study may not play a leading role. In summary, the analytical results of the formation mechanism of nitrate on the trip from East Asia to the North Pole in the process from outside the Arctic Circle to the inside of the Arctic Circle, and then on the return journey from the North Pole in the process from inside the Arctic Circle to outside the Arctic Circle (Supplementary Fig. 5a–d) show that the contribution of the $NO_2 + OH$ pathway increases with increasing daytime length and then decreases with decreasing daytime length, further suggesting that the large latitudinal variation of $\Delta^{17}O\text{-}NO_3^-$ observed may be due to the time gap between daytime and nighttime.

Based on the $\Delta^{17}O\text{-}NO_3^-$ observed from East Asia to the Arctic Ocean, this study provides valuable insights into the special mechanisms of nitrate formation in the marine atmosphere of the Arctic Ocean, which is crucial for understanding the impact of sea ice on the Arctic environment. Our findings confirm that the recently observed abnormally low $\Delta^{17}O\text{-}NO_3^-$ values in the Arctic Ocean were not accidental and provide evidence for the effect of sea ice on atmospheric oxidizability. $\Delta^{17}O\text{-}NO_3^-$ values showed a clear negative trend with both latitude and day length. During the permanent sunlight period, the $\Delta^{17}O\text{-}NO_3^-$ values were extremely low and decreased significantly with increasing latitude, which aligns with the simulated sea ice cover area. The effect of sea ice has been shown to enhance the production of OH and peroxy radicals, and this could make the ratio of peroxy radical oxidation to form NO_2 likely higher than expected, resulting in lower $\Delta^{17}O\text{-}NO_2$ values than expected. This then acted in conjunction with the $NO_2 + OH$ pathway to cause the observed low $\Delta^{17}O\text{-}NO_3^-$. The increase in $\Delta^{17}O\text{-}NO_3^-$ of the same latitude oceanic range on the return trip could be attributed to the contribution of the high-$\Delta^{17}O$ (NO_3 related) pathways at night due to the longer nighttime at the return trip.

Our study highlights the need for further research to better understand the formation mechanisms of nitrate in the Arctic marine atmosphere. Specifically, to better match the lower $\Delta^{17}O\text{-}NO_3^-$ of the Arctic Ocean in this study, we recommend investigating the chemical enhancement of peroxy radicals in the upper atmosphere of the sea ice-covered ocean during the permanent sunlight phase. These findings could help to improve our understanding of the impact of sea ice of Arctic environment. Furthermore, this work shows that $\Delta^{17}O\text{-}NO_3^-$ values can reflect changes in oxidants within the NO_x cycle and $\Delta^{17}O\text{-}NO_3^-$ may be used to improve global atmospheric chemical models. In the future, more attention should be paid to the observation and simulation research on the $\Delta^{17}O$ of NO_2, and the A value (the proportion of NO_2 produced by ozone oxidation) should be corrected more accurately.

METHODS

Cruise description of R/V Xuelong

In 2017, the Chinese R/V Xuelong cruise successfully passed the Trans-Arctic Channel during the eighth China Arctic Expedition, which was the first successful trial of a Chinese ship on the

Northwest Passage of the Arctic. On July 20, 2017, the R/V Xuelong set sail from the Shanghai Wharf of the Chinese Polar Research Institute (121.69°E, 31.32°N), crossed the Sea of Japan, and crossed the Bering Strait to the Arctic Circle on July 31. The R/V Xuelong passed through the highest latitude sea area at around 86°N on or around August 13. By August 19, the ship had begun a clockwise circumnavigation of Greenland, viewed from the North Pole, before returning and passing through the Arctic Bay and the waters of western Canada. It wasn't until September 24 that the R/V Xuelong completely exited the Arctic Circle, and it returned until October 10.

Collection for aerosol samples

The cruise trajectories of R/V Xuelong and the locations of sampling points are shown in Supplementary Fig. 7. The total suspended particulate matter (TSP) was collected by the large-flow sampler ASM-1 (Mingye, Guangzhou, China) at 700 L/min on R/V Xuelong. A total of 34 48 hour-TSP samples and 1 blank sample were collected. The sampler set was installed on the deck of the ship about 10 m from the sea level. The machine was closed when the ship is just sailing and other times when it is not suitable for sampling to avoid contamination by the ship's exhaust gas. The onboard monitoring system recorded real-time information such as latitude and longitude, temperature, humidity, and wind speed. Information about the location of the sampling point and the meteorological conditions is shown in Supplementary Table 4.

All samples were collected on quartz filters (size 8×10 in, Pallflex). Before sampling, the filter was wrapped in aluminum foil and baked in a muffle furnace at 450 °C for 6 h to remove impurities. After sampling, the filter was placed in clean aluminum foil and stored in a refrigerator at −26 °C until chemical and isotope analysis was performed.

Chemistry and isotope analysis

The 3.14 cm^2 filter cut from the quartz filter was immersed in a 15 mL vial containing 10 mL ultrapure water (18.2 MΩ). After 30 min of ultrasonic vibration and filtration, inorganic ions mainly including Na^+, K^+, Mg^{2+}, Ca^{2+}, NH_4^+, Cl^-, NO_3^-, SO_4^{2-} etc. were measured by ion chromatograph (ICS 5000+, Thermo Scientific, USA). Each batch of samples contains blank samples and water blanks. The detection limit of NO_3^- is 0.005 μg/ml. The correlation coefficient of the calibration curve of each batch of samples reached 0.999.

Oxygen isotopes of nitrate were determined using the denitrifying bacteria method, which can be found elsewhere[53]. Nitrate is converted into N_2O gas by denitrifying bacteria (Pseudomonas aureus, ATCC13985), and N_2 and O_2 are generated by pyrolysis of a gold tube at 800 °C. The $\Delta^{17}O$ (obtained by measuring $\delta^{17}O$ and $\delta^{18}O$ of O_2, $\Delta^{17}O = \delta^{17}O - 0.52 \times \delta^{18}O$) was measured by using an isotope ratio mass spectrometer (MAT253, Thermo Scientific, USA). The detection limit of this method is 0.4 μgN. The verification of international standard samples (USGS34, USGS35, and IAEA-NO-3) showed that the analytical accuracy of $\Delta^{17}O$ can reach 0.19‰ and the uncertainties values were 0.3 ‰. Meanwhile, every 10 samples were accompanied by a replicate, and the standard deviation of $\Delta^{17}O$ between the replicates was 0.5‰.
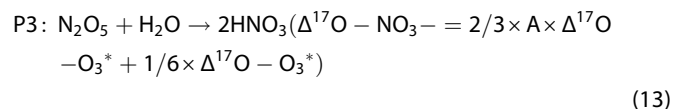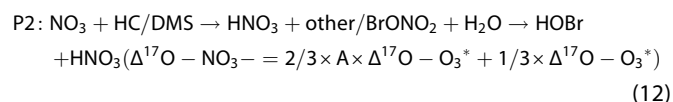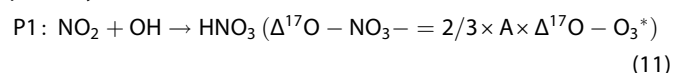
Backward trajectory analysis

The backward trajectory is the analysis of the source and transport path of the air mass based on the path of the atmospheric air mass moving in a certain period of time. The 5-day air mass backward trajectory during the whole sampling was calculated using TrajStat[54] to study the long-distance transmission of pollutants, with the set of 1000 m above sea level. The global data assimilation system GDAS data provided by the US Air Resources Laboratory (NOAA ARL) was used. The result is shown in Supplementary Fig. 2.

The stations near the coast were greatly affected by continental air mass, while the distant sea was less affected.

Quantification of Nitrate Formation Pathways

The simulation of global nitrate formation pathways of Alexander et al.[28] showed that nitrate formation is mainly through OH (Eq. (4) ~ 41%) and N_2O_5 (Eq. (8) ~ 41%) pathways. In addition, the oxidative halogen XO pathway (Eq. (9) ~ 6%) and $NO_3 + HC$ (Eq. (6) ~ 4%) contributed the most. However, many studies do not consider the XO pathway. Halogen bromine chemistry (X=Br) is considered in this study because the main sources of active halogen in the troposphere are sea salt aerosols and seawater[55]. Here we assume that the $\Delta^{17}O$ of OH, HO_2 and RO_2 is about 0‰, which is consistent with other studies[10,21] (Supplementary Note 1). Therefore, it can be inferred that the nitrate formed by the reaction of O_3 and XO has a higher $\Delta^{17}O$ while formed related HO_2, RO_2, OH, and H_2O have lower values. The $\Delta^{17}O$ of nitrate is determined by the $\Delta^{17}O$ of NO_2 and the conversion process of NO_2 to nitrate. The $\Delta^{17}O$ value of NO_2 should be expressed as $A \times \Delta^{17}O\text{-}O_3^*$, where the value of A represents the relative importance of the oxidation pathway in which NO is oxidized to NO_2 (where the transferred oxygen atoms come from ozone ($NO + O_3$ and $NO + XO$)) and $\Delta^{17}O\text{-}O_3^*$ represents the $\Delta^{17}O$ of the oxygen atom transferred by O_3. Theoretical $\Delta^{17}O\text{-}NO_3^-$ values calculated for each formation pathway were shown in Supplementary Table 3 based on Supplementary Note 1, in summary, the nitrate formation reactions are divided according to $\Delta^{17}O$ into three main pathways P1, P2, P3:

$$P1: NO_2 + OH \rightarrow HNO_3 \, (\Delta^{17}O - NO_3- = 2/3 \times A \times \Delta^{17}O - O_3^*)$$
(11)

$$P2: NO_3 + HC/DMS \rightarrow HNO_3 + other/BrONO_2 + H_2O \rightarrow HOBr$$
$$+ HNO_3(\Delta^{17}O - NO_3- = 2/3 \times A \times \Delta^{17}O - O_3^* + 1/3 \times \Delta^{17}O - O_3^*)$$
(12)

$$P3: N_2O_5 + H_2O \rightarrow 2HNO_3(\Delta^{17}O - NO_3- = 2/3 \times A \times \Delta^{17}O$$
$$-O_3^* + 1/6 \times \Delta^{17}O - O_3^*)$$
(13)

Therefore, $\Delta^{17}O\text{-}NO_3^- = P1 \times f1 + P2 \times f2 + P3 \times f3$, where f represents the relative contribution of each pathway, and $f1 + f2 + f3 = 1$.

The contribution of different formation pathways was quantitatively analyzed using the SIAR (Stable Isotope Analysis in R) model (Supplementary Note 3). The average and the standard deviation value of $\Delta^{17}O\text{-}NO_3^-$ of each pathway were input into SIAR. Finally, the estimated values of f1, f2, and f3 can be obtained.

REFERENCES
1. Wolff E. W. Nitrate in Polar Ice. In: Ice Core Studies of Global Biogeochemical Cycles. NATO ASI Series, Vol 30 (Springer Berlin, Heidelberg, 1995).

2. Blaszczak-Boxe, C. S. & Saiz-Lopez, A. Nitrate photolysis in ice and snow: A critical review of its multiphase chemistry. *Atmos. Environ.* **193**, 224–241 (2018).

3. Savarino, J. et al. Isotopic composition of atmospheric nitrate in a tropical marine boundary layer. *Proc. Natl. Acad. Sci.* **110**, 17668–17673 (2013).

4. Fan, M. Y. et al. Important Role of NO$_3$ Radical to Nitrate Formation Aloft in Urban Beijing: Insights from Triple Oxygen Isotopes Measured at the Tower. *Environ. Sci. Technol.* **56**, 6870–6879 (2021).

5. He, P. et al. Atmospheric $\Delta^{17}O(NO_3^-)$ reveals nocturnal chemistry dominates nitrate production in Beijing haze. *Atmos. Chem. Phys.* **18**, 14465–14476 (2018).

6. He, P. et al. The observation of isotopic compositions of atmospheric nitrate in Shanghai China and its implication for reactive nitrogen chemistry. *Sci. Total Environ.* **714**, 136727 (2020).

7. Lin, Y. C. et al. Formation Mechanisms and Source Apportionments of Airborne Nitrate Aerosols at a Himalayan-Tibetan Plateau Site: Insights from Nitrogen and Oxygen Isotopic Compositions. *Environ. Sci. Technol.* **55**, 12261–12271 (2021).

8. Song, W. et al. Nitrogen isotope differences between atmospheric nitrate and corresponding nitrogen oxides: a new constraint using oxygen isotopes. *Sci. Total Environ.* **701**, 134515 (2020).

9. Sofen, E. et al. WAIS Divide ice core suggests sustained changes in the atmospheric formation pathways of sulfate and nitrate since the 19th century in the extratropical Southern Hemisphere. *Atmos. Chem. Phys.* **14**, 5749–5769 (2014).

10. Alexander, B. et al. Quantifying atmospheric nitrate formation pathways based on a global model of the oxygen isotopic composition ($\Delta^{17}O$) of atmospheric nitrate. *Atmos. Chem. Phys.* **9**, 5043–5056 (2009).

11. Carter, T. S., Joyce, E. E. & Hastings, M. G. Quantifying Nitrate Formation Pathways in the Equatorial Pacific Atmosphere from the GEOTRACES Peru-Tahiti Transect. *ACS Earth Space Chem.* **5**, 2638–2651 (2021).

12. Kamezaki, K. et al. Nitrogen and Triple Oxygen Isotopic Analyses of Atmospheric Particulate Nitrate over the Pacific Ocean. (*EGU General Assembly Conference Abstracts*, 2017).

13. Gobel, A. R., Altieri, K. E., Peters, A. J., Hastings, M. G. & Sigman, D. M. Insights into anthropogenic nitrogen deposition to the North Atlantic investigated using the isotopic composition of aerosol and rainwater nitrate. *Geophys. Res. Lett.* **40**, 5977–5982 (2013).

14. Crutzen, P. J. The influence of nitrogen oxides on the atmospheric ozone content. *Q. J. R. Meteorol. Soc.* **96**, 320–325 (1970).

15. Scarratt, M. et al. Influence of phytoplankton taxonomic profile on the distribution of dimethylsulfide and dimethylsulfoniopropionate in the northwest Atlantic. *Mar. Ecol. Prog. Ser.* **244**, 49–61 (2002).

16. Peng, X. et al. An unexpected large continental source of reactive bromine and chlorine with significant impact on wintertime air quality. *Natl Sci. Rev.* **8**, nwaa304 (2021).

17. Li, Q. et al. Halogens enhance haze pollution in China. *Environ. Sci. Technol.* **55**, 13625–13637 (2021).

18. Kamezaki, K. et al. Tracing the sources and formation pathways of atmospheric particulate nitrate over the Pacific Ocean using stable isotopes. *Atmos. Environ.* **209**, 152–166 (2019).

19. Morin, S., Savarino, J., Bekki, S., Gong, S. & Bottenheim, J. Signature of Arctic surface ozone depletion events in the isotope anomaly ($\Delta^{17}O$) of atmospheric nitrate. *Atmos. Chem. Phys.* **7**, 1451–1469 (2007).

20. Patris, N., Cliff, S., Quinn, P., Kasem, M. & Thiemens, M. Isotopic analysis of aerosol sulfate and nitrate during ITCT-2k2: Determination of different formation pathways as a function of particle size. *J. Geophys. Res.* **112**, D23301 (2007).

21. Michalski, G., Scott, Z., Kabiling, M. & Thiemens, M. H. First measurements and modeling of $\Delta^{17}O$ in atmospheric nitrate. *Geophys. Res. Lett.* **30**, 1870 (2003).

22. Shi, G. et al. Using stable isotopes to distinguish atmospheric nitrate production and its contribution to the surface ocean across hemispheres. *Earth Planet. Sci. Lett.* **564**, 116914 (2021).

23. Savarino, J., Bhattacharya, S., Morin, S., Baroni, M. & Doussin, J. F. The NO+O$_3$ reaction: A triple oxygen isotope perspective on the reaction dynamics and atmospheric implications for the transfer of the ozone isotope anomaly. *J. Chem. Phys.* **128**, 194303 (2008).

24. Savarino, J. & Thiemens, M. H. Mass-independent oxygen isotope (^{16}O, ^{17}O, ^{18}O) fractionation found in H$_x$, O$_x$ reactions. *J. Chem. Soc. A* **103**, 9221–9229 (1999).

25. Li, Y. et al. Significant latitudinal gradient of nitrate production in the marine atmospheric boundary layer of the Northern Hemisphere. *Geophys. Res. Lett.* **49**, e2022GL100503 (2022).

26. Guha, T. et al. Isotopic ratios of nitrate in aerosol samples from Mt. Lulin, a high-altitude station in Central Taiwan. *Atmos. Environ.* **154**, 53–69 (2017).

27. Xia, X. et al. Triple oxygen isotopic evidence for atmospheric nitrate and its application in source identification for river systems in the Qinghai-Tibetan Plateau. *Sci. Total Environ.* **688**, 270–280 (2019).

28. Alexander, B. et al. Global inorganic nitrate production mechanisms: comparison of a global model with nitrate isotope observations. *Atmos. Chem. Phys.* **20**, 3859–3877 (2020).

29. Yu, C. et al. Characteristics of aerosol WSI with high-time-resolution observation over Arctic Ocean. *Earth Space Sci.* **7**, e2020EA001227 (2020).

30. Morin, S. et al. Tracing the origin and fate of NO$_x$ in the Arctic atmosphere using stable isotopes in nitrate. *Science* **322**, 730–732 (2008).

31. Burger, J. M. et al. The importance of alkyl nitrates and sea ice emissions to atmospheric NO$_x$ sources and cycling in the summertime Southern Ocean marine boundary layer. *Atmos. Chem. Phys.* **22**, 1081–1096 (2022).

32. Vicars, W. et al. Spatial and diurnal variability in reactive nitrogen oxide chemistry as reflected in the isotopic composition of atmospheric nitrate: Results from the CalNex 2010 field study. *J. Geophys. Res.: Atmos.* **118**, 10567–10588 (2013).

33. Kettle, A. et al. A global database of sea surface dimethylsulfide (DMS) measurements and a procedure to predict sea surface DMS as a function of latitude, longitude, and month. *Glob. Biogeochem. Cycles* **13**, 399–444 (1999).

34. Manktelow, P., Mann, G., Carslaw, K., Spracklen, D. & Chipperfield, M. Regional and global trends in sulfate aerosol since the 1980s. *Geophys. Res. Lett.* **34**, (2007).

35. Jiang, B. et al. Effects of atmospheric oxidation processes on the latitudinal distribution differences in MSA and nss-SO$_4^{2-}$ in the Northwest Pacific. *Atmos. Environ.* **298**, 119618 (2023).

36. Prospero, J. M., Savoie, D. L. & Arimoto, R. Long-term record of nss-sulfate and nitrate in aerosols on Midway Island, 1981–2000: Evidence of increased (now decreasing?) anthropogenic emissions from Asia. *J. Geophys. Res. Atmos.* **108**, AAC 10-11-AAC 10–11 (2003).

37. Morin, S. et al. Major influence of BrO on the NO$_x$ and nitrate budgets in the Arctic spring, inferred from $\Delta^{17}O$ (NO$_3^-$) measurements during ozone depletion events. *Environ. Chem.* **4**, 238–241 (2007).

38. Halfacre, J. et al. Temporal and spatial characteristics of ozone depletion events from measurements in the Arctic. *Atmos. Chem. Phys.* **14**, 4875–4894 (2014).

39. Abbatt, J. et al. Halogen activation via interactions with environmental ice and snow in the polar lower troposphere and other regions. *Atmos. Chem. Phys.* **12**, 6237–6271 (2012).

40. Mu, L., Liang, X., Yang, Q., Liu, J. & Zheng, F. Arctic Ice Ocean Prediction System: evaluating sea-ice forecasts during Xuelong's first trans-Arctic Passage in summer 2017. *J. Glaciol.* **65**, 813–821 (2019).

41. Berhanu, T. et al. Isotopic effects of nitrate photochemistry in snow: a field study at Dome C, Antarctica. *Atmos. Chem. Phys.* **15**, 11243–11256 (2015).

42. Geng, L. et al. Isotopic evidence of multiple controls on atmospheric oxidants over climate transitions. *Nature* **546**, 133–136 (2017).

43. Boxe, C. et al. Kinetics of NO and NO$_2$ evolution from illuminated frozen nitrate solutions. *J. Phys. Chem. A* **110**, 3578–3583 (2006).

44. Berhanu, T. A. et al. Laboratory study of nitrate photolysis in Antarctic snow. II. Isotopic effects and wavelength dependence. *J. Phys. Chem.* **140**, 244306 (2014).

45. Clark, S., Granger, J., Mastorakis, A., Aguilar-Islas, A. & Hastings, M. An investigation into the origin of nitrate in Arctic Sea ice. *Glob. Biogeochem. Cycles* **34**, e2019GB006279 (2020).

46. Brough, N., Jones, A. E. & Griffiths, P. T. Influence of sea ice-derived halogens on atmospheric HO$_x$ as observed in springtime coastal Antarctica. *Geophys. Res. Lett.* **46**, 10168–10176 (2019).

47. Ahmed, S. et al. The Role of Snow in Controlling Halogen Chemistry and Boundary Layer Oxidation During Arctic Spring: A 1D Modeling Case Study. *J. Geophys. Res.: Atmos.* **127**, e2021JD036140 (2022).

48. Oldridge TNW. Halogen activation from sea ice: Nitrate photolysis and heterogeneous reaction with ozone. (University of Toronto, 2009).

49. Geng, L. et al. On the origin of the occasional spring nitrate peak in Greenland snow. *Atmos. Chem. Phys.* **14**, 13361–13376 (2014).

50. Liao, J. et al. Observations of hydroxyl and peroxy radicals and the impact of BrO at Summit, Greenland in 2007 and 2008. *Atmos. Chem. Phys.* **11**, 8577–8591 (2011).

51. Morin, S. et al. Comprehensive isotopic composition of atmospheric nitrate in the Atlantic Ocean boundary layer from 65 S to 79 N. *J. Geophys. Res.: Atmos.* **114**, D05303 (2009).

52. Lehrer, E., Hönninger, G. & Platt, U. A one dimensional model study of the mechanism of halogen liberation and vertical transport in the polar troposphere. *Atmos. Chem. Phys.* **4**, 2427–2440 (2004).

53. Yu, H. R., Cao, F., Zhang, W. Q., Zhao, Z. Y. & Zhang, Y. L. Determination of ^{17}O Anomaly in Atmospheric Aerosol Nitrate. *Chin. J. Anal. Chem.* **49**, 253–262 (2021).

54. Wang, Y., Zhang, X. & Draxler, R. R. TrajStat: GIS-based software that uses various trajectory statistical analysis methods to identify potential sources from long-term air pollution measurement data. *Environ. Modell. Softw.* **24**, 938–939 (2009).

55. Wang, X. et al. The role of chlorine in global tropospheric chemistry. *Atmos. Chem. Phys.* **19**, 3981–4003 (2019).

AUTHOR CONTRIBUTIONS

Y.Z. designed the study. Z.Z., Y.Z., and F.C. conceived and organized this paper. Z.Z. conducted the measurement of oxygen isotopes, with contributions from H.Y., H.L., and M.F. to laboratory experiments. Z.Z. and Y.H. conducted the back trajectory simulation. Z.Z. and Y.Z. prepared the manuscript with contributions from W.S., Y.L., and M.G.; All authors reviewed and commented on the final manuscript.

COMPETING INTERESTS

The authors declare no competing interests.

ADDITIONAL INFORMATION

Supplementary information The online version contains supplementary material available at https://doi.org/10.1038/s41612-023-00447-7.

Correspondence and requests for materials should be addressed to Yanlin Zhang.

Reprints and permission information is available at http://www.nature.com/reprints

Publisher's note Springer Nature remains neutral with regard to jurisdictional claims in published maps and institutional affiliations.